



Integrative Transcriptomic Profiling and Network-Based Analysis Reveal Disease-Specific and Shared Molecular Pathways Across Five Major Ocular Disorders

Siamak Salimy¹

¹Department of Computer Engineering, National University of Skills (NUS), Tehran, Iran

Received: 2025/11/02 Accepted: 2025/12/05 Online Published: 2025/12/05

Abstract

Ocular diseases constitute a heterogeneous group of conditions that collectively cause significant visual impairment and blindness. Despite advances in clinical diagnostics, the molecular mechanisms driving ocular pathology remain insufficiently understood. This study sought to systematically investigate transcriptional dysregulation across five distinct ocular disorders by integrating multi-cohort gene expression datasets. Five microarray datasets from the Gene Expression Omnibus (GEO, GSE137996 (Congenital Aniridia, n=12), GSE17549 (Choroideremia, n=14), GSE112201 (Corneal Dystrophy, n=20), GSE9944 (Glaucoma, n=10), and GSE29801 (Macular Degeneration, n=12)) were processed using a standardized pipeline involving background correction, normalization, and gene-level filtering. Differential expression analysis was performed with Limma, and significance was determined using the Benjamini–Hochberg FDR correction, $\text{adj-p-value} < 0.05$, and $\log_2\text{FC}$ threshold ($|\log_2\text{FC}| > 1$). Protein–protein interaction (PPI) networks were constructed using STRING and analyzed in Cytoscape, while GO and KEGG enrichment analyses were conducted using Enrichr. Distinct transcriptional signatures were identified across the five disorders, including 112 DEGs in congenital aniridia, 21 in choroideremia, 812 in corneal dystrophy, 32 in glaucoma, and 17 in macular degeneration. PPI networks revealed prominent disease-specific functional clusters, including developmental regulation in aniridia, retinal metabolic pathways in choroideremia, inflammatory and extracellular matrix remodeling pathways in corneal dystrophy, neurodegenerative processes in glaucoma, and oxidative stress responses in macular degeneration. Cross-dataset comparisons highlighted shared molecular themes, including immune activation, stress-response signaling, and extracellular matrix dysregulation. This integrative systems-level analysis provides a comprehensive molecular framework for understanding major ocular disorders. The identification of key regulatory hubs, disease-specific pathways, and shared pathogenic mechanisms offers new perspectives for the development of precision biomarkers and targeted therapeutic strategies. These findings enhance the current molecular understanding of ocular disease biology and establish a scalable analytical foundation for future multi-omics investigations.

Keywords: Ocular disease gene expression analysis, Differentially expressed genes in eye disorders, Ocular biomarker discovery, Transcriptomic profiling of ocular diseases, Molecular pathways in ocular disorders.

Cite this article: Salimy S. Integrative Transcriptomic Profiling and Network-Based Analysis Reveal Disease-Specific and Shared Molecular Pathways Across Five Major Ocular Disorders. *Informatics in Biology, Health, and Food*. 2025;2(2):99-119.

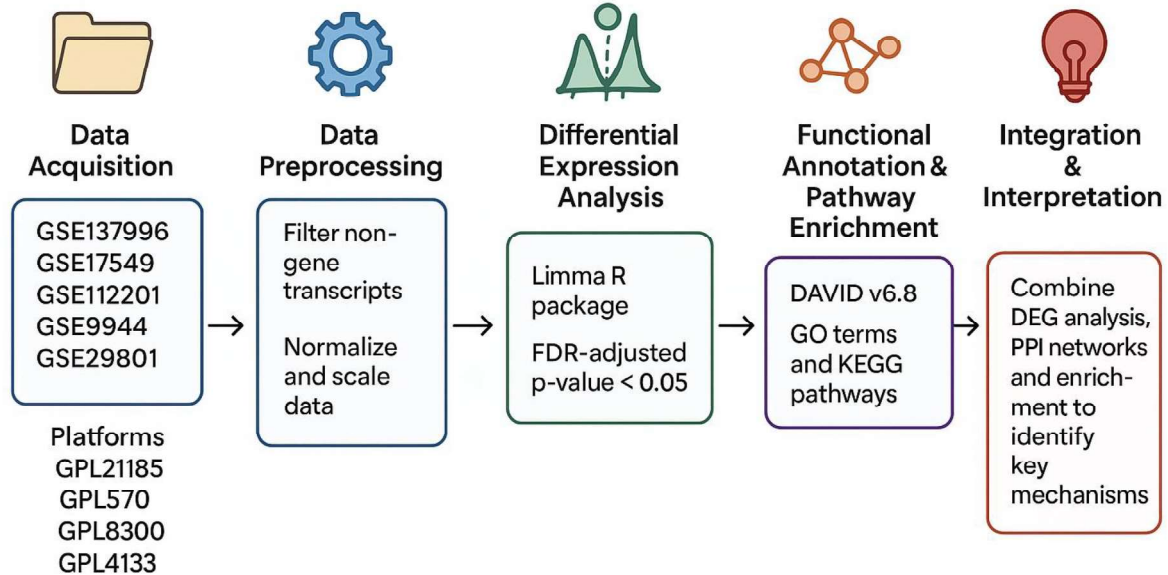
Copyright©: The Authors. Published by Shandiz Institute of Higher Education

Corresponding authors: Siamak Salimy

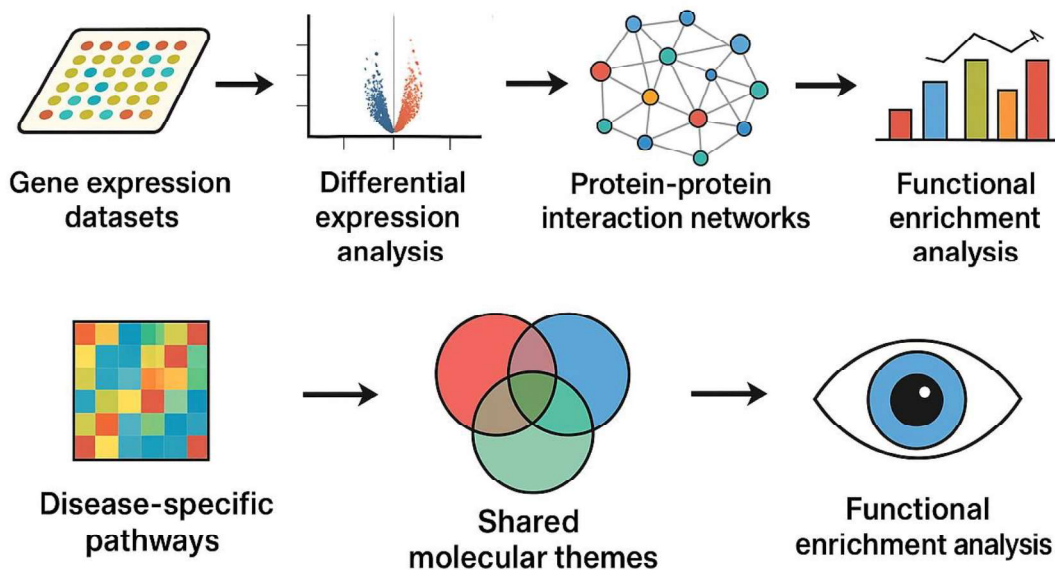
Email: salimy@ut.ac.ir



Comprehensive Analysis of Differentially Expressed Genes Across Ocular Disorders



Integrative Transcriptomic Profiling and Network-Based Analysis Reveal Disease-Specific and Shared Molecular Pathways Across Five Major Ocular Disorders



Introduction

Ocular disorders represent a heterogeneous group of conditions that collectively account for a significant proportion of global visual impairment and irreversible blindness (1). Although clinical diagnostics and therapeutic interventions have advanced, the molecular mechanisms underlying the onset, progression, and phenotypic diversity of ocular diseases remain insufficiently characterized (2). Elucidating these mechanisms requires integrative approaches that capture the complexity of gene regulatory alterations across diverse disease contexts (3). High-throughput transcriptomic profiling has facilitated systematic exploration of genome-wide expression dynamics, providing a robust framework for identifying pathological drivers, molecular biomarkers, and potential therapeutic targets (4).

Public repositories such as the NCBI Gene Expression Omnibus (GEO) enable the collection of large-scale transcriptomic data across diverse biological conditions, technological platforms, and patient populations (5). Leveraging such datasets enhances the statistical power of molecular discovery and facilitates cross-disease comparisons, uncovering both shared regulatory programs and disease-specific transcriptional patterns. In this study, five GEO datasets were systematically analyzed: GSE137996, GSE17549, GSE112201, GSE9944, and GSE29801. These datasets encompass phenotypically and genetically distinct eye disorders, including congenital aniridia (6), choroideremia (CHM)(7), corneal dystrophy (CD) (8), glaucoma(9), and macular degeneration (MD) (10). The datasets were generated using high-resolution microarray platforms, including Agilent SurePrint G3 and Affymetrix U133 and U95 arrays, enabling a comprehensive examination of the ocular transcriptome.

By integrating multi-cohort differential expression profiling, network biology, and pathway enrichment analyses, this study provides a comprehensive overview of transcriptional changes in major eye disorders, highlighting both shared and disease-specific

molecular mechanisms that may inform future diagnostic and therapeutic strategies.

Methods

Data Retrieval and Dataset Selection

Five publicly available gene expression datasets were retrieved from the NCBI Gene Expression Omnibus (GEO) database. The datasets—GSE137996, GSE17549, GSE112201, GSE9944, and GSE29801—were selected to represent a broad spectrum of ocular disorders, including congenital aniridia, choroideremia (CHM), corneal dystrophy (CD), glaucoma, and macular degeneration (MD). These datasets were generated on multiple microarray platforms, namely GPL21185 (Agilent-072363 SurePrint G3 Human GE v3 8×60K), GPL570 (Affymetrix Human Genome U133 Plus 2.0 Array), GPL8300 (Affymetrix Human Genome U95 Version 2 Array), and GPL4133 (Agilent-014850 Whole Human Genome 4×44K G4112F). For each dataset, raw expression files and corresponding platform annotation data were downloaded for further analysis. Sample Characteristics for each GEO Dataset are listed in Table 1.

Preprocessing and Quality Control

Standardized preprocessing pipelines were applied to ensure cross-platform comparability. For Affymetrix datasets (GPL570 and GPL8300), raw CEL files were imported into R using the *affy* and *oligo* packages. (11). Background correction, within-array normalization, and probe summarization were performed via the Robust Multi-array Average (RMA) algorithm. Agilent datasets (GPL21185 and GPL4133) were processed using the *limma* package, employing background correction with the “normexp” method and within-array normalization using “loess.” (12).

To ensure biological relevance, non-gene transcripts, control probes, and unannotated features were removed using the platform annotation tables. Following filtering, all datasets were log₂-transformed, quantile-normalized, and scaled to minimize technical variability. Quality control was assessed using density plots, boxplots, and principal component analysis (PCA) to confirm uniformity and detect

Table 1. Sample Characteristics for Five GEO Datasets.

Dataset (GSE ID)	Disease Type	Tissue Source	Platform (GPL)	Cases (n)	Controls (n)	Total Samples
GSE137996	Congenital Aniridia	Retina	GPL21185 (Agilent G3 8×60K)	6	6	12
GSE17549	Choroideremia (CHM)	Retina / RPE	GPL570 (Affymetrix U133 Plus 2.0)	7	7	14
GSE112201	Corneal Dystrophy (CD)	Cornea	GPL4133 (Agilent 4×44K)	10	10	20
GSE9944	Glaucoma	Optic Nerve Head / Retina	GPL8300 (Affymetrix U95 v2)	5	5	10
GSE29801	Macular Degeneration (MD)	Retina (Macula)	GPL570 (Affymetrix U133 Plus 2.0)	6	6	12

outliers. No samples were excluded based on QC metrics, as all showed consistent clustering in PCA and no extreme expression outliers in boxplots. However, due to the small sample sizes, potential confounding effects of age and sex could not be fully evaluated, as this information was not consistently available in the original dataset submissions.

Differential Gene Expression Analysis

Differential expression analysis was carried out using the Limma (Linear Models for Microarray Data) package from the Bioconductor project. For each dataset, linear models were fitted to assess expression differences between disease groups and their respective controls. Empirical Bayes moderation was applied to stabilize variance estimates across genes (12).

To correct for multiple hypothesis testing, p-values were adjusted using the Benjamini–Hochberg false discovery rate (FDR) method. (13) Genes with an adjusted p-value < 0.05 were considered significantly differentially expressed (DEGs) and retained for downstream analysis. DEG counts for each dataset were recorded to evaluate disease-specific transcriptional activity.

Protein–Protein Interaction (PPI) Network Construction

To investigate functional interactions among DEGs, protein–protein interaction networks

were constructed using the STRING database (version 12.0) (14). DEG lists from each dataset were uploaded to STRING, and networks were generated using a high-confidence interaction threshold (combined score ≥ 0.7) to ensure reliability. Only experimentally validated, data base-curated, and high-confidence predicted interactions were included.

Networks were exported and visualized in Cytoscape (version 3.8.2). (15) Network topology parameters—including degree centrality, betweenness centrality, closeness, and clustering coefficient—were used to identify hub genes and functional modules.

Functional Enrichment and Pathway Analysis

Functional interpretation of the DEGs and PPI clusters was performed using the enrichr package (16). Enrichment analyses encompassed: Gene Ontology (GO), Biological Process (BP), GO Cellular Component (CC), GO Molecular Function (MF), Kyoto Encyclopedia of Genes and Genomes (KEGG) pathways (17)

Terms with $FDR < 0.1$ were deemed significantly enriched. Enrichment plots were used to identify disease-specific pathways and shared biological mechanisms across datasets. Graphical representations of enriched GO terms and KEGG pathways were generated in R.

Visualization and Data Integration

Results of differential expression analyses were visualized using volcano plots, generated with the *ggplot2* package to highlight statistically significant gene expression changes. (18) PPI networks and enrichment results were integrated to construct a multi-layered systems biology map for each ocular condition. Comparative integration across datasets was performed to identify shared molecular pathways, unique disease-specific signatures, and potentially targetable regulatory hubs.

Reproducibility and Computational Environment

All analyses were conducted in R version 4.3.x using Bioconductor packages.(19). Cytoscape networks were generated in Cytoscape 3.8.2. To ensure reproducibility, all scripts, parameter settings, and workflow steps were recorded and validated across datasets. (20)

To ensure analytical rigor and comparability, all datasets underwent a standardized preprocessing workflow that included gene-level filtering, normalization, and variance stabilization. (21) Differential expression analysis was performed using the Limma framework, an empirical Bayes method optimized for microarray data. Statistical significance was determined using the Benjamini–Hochberg false discovery rate (FDR) procedure to control for multiple testing. (12) The analysis revealed substantial variability in transcriptional dysregulation across diseases, with 112 differentially expressed genes (DEGs) identified in congenital aniridia, 21 in CHM, 812 in CD, 32 in glaucoma, and 17 in MD. These findings reflect the distinct biological underpinnings and disease progression associated with each condition. (22)

To interpret gene-level changes in terms of underlying mechanisms, protein-protein interaction (PPI) networks were constructed using the STRING database (version 12.0) with a stringent interaction score cutoff of 0.7. PPI network modeling facilitates the identification of key genes, interaction clusters, and principal signaling pathways that regulate disease-related processes. Cytoscape was employed for network visualization and topological refinement,

providing a systems-level perspective on the molecular architecture of each disease. (23)

Results

Differential Gene Expression Analysis Across Five Ocular Disorders

Differential expression analysis was performed on five independent GEO datasets representing distinct ocular diseases (GSE137996, GSE17549, GSE112201, GSE9944, and GSE29801). After preprocessing, normalization, and filtering of non-gene transcripts, each dataset yielded a unique transcriptional signature reflective of its underlying pathology.

A total of 112 DEGs were identified in congenital aniridia (GSE137996), 21 DEGs in choroideremia (GSE17549), 812 DEGs in corneal dystrophy (GSE112201), 32 DEGs in glaucoma (GSE9944), and 17 DEGs in macular degeneration (GSE29801). The magnitude of these differences underscores the heterogeneity of transcriptional dysregulation among ocular conditions.

Volcano plots for each dataset revealed clear separation between significantly upregulated and downregulated genes, indicating robust differential expression signals across all disease states (Figure 1). Notably, the CD dataset exhibited the most extensive transcriptional perturbation, consistent with the prominent inflammatory and structural remodeling processes characterizing corneal pathology. Differentially Expressed Genes Across Five Ocular Disorders are listed in Table 2.

Protein–Protein Interaction (PPI) Network Construction Reveals Distinct Disease-Specific Functional Modules

To investigate functional connectivity among DEGs, PPI networks were constructed using STRING (interaction scores ≥ 0.7) and visualized in Cytoscape. Each network exhibited distinct topological features and hub gene profiles reflective of disease-specific biological mechanisms (Figure 2).

Other criteria for STRING network construction are: Network type: complete STRING network (the edges indicate both functional and physical protein associations). Meaning of network

Table 2. Differentially Expressed Genes Across Five Ocular Disorders.

Dataset	Disease	Upregulated Genes	Downregulated Genes	Total DEGs (FDR < 0.1)
GSE137996	Congenital Aniridia	59	53	112
GSE17549	Choroideremia (CHM)	10	11	21
GSE112201	Corneal Dystrophy (CD)	410	402	812
GSE9944	Glaucoma	15	17	32
GSE29801	Macular Degeneration (MD)	9	8	17

edges: evidence. Active interaction sources: Text mining, Experiments, Databases, Co-expression, Neighborhood, Gene Fusion, and Co-occurrence. In congenital aniridia, the PPI network identified a cluster of genes implicated in developmental regulation, transcriptional control, and ocular morphogenesis, consistent with the disorder's congenital and structural nature. In CHM, the small but cohesive network centered on genes involved in retinal metabolic pathways and photoreceptor maintenance aligns with the progressive degeneration characteristic of choroideremia.

The CD dataset generated a highly interconnected network with several high-degree nodes representing immune response regulators, extracellular matrix proteins, and pro-inflammatory mediators. This finding corresponds with the broad DEG profile and reflects the critical role of inflammation in corneal dystrophy. Glaucoma networks revealed clusters associated with neurodegeneration, apoptosis regulation, and intraocular pressure-related mechanisms, consistent with retinal ganglion cell loss. In MD, the network showed connections among genes participating in oxidative stress responses, cellular homeostasis, and tissue degeneration, reflecting the multifactorial nature of macular deterioration. corresponds with the broad DEG profile and reflects the critical role of inflammation in corneal dystrophy. Glaucoma networks revealed clusters associated with neurodegeneration, apoptosis regulation, and intraocular pressure-related mechanisms, consistent with retinal ganglion cell loss. In MD, the network showed connections among genes

participating in oxidative stress responses, cellular homeostasis, and tissue degeneration, reflecting the multifactorial nature of macular deterioration. with the disorder's congenital and structural nature. In CHM, the small but cohesive network centered on genes involved in retinal metabolic pathways and photoreceptor maintenance aligns with the progressive degeneration characteristic of choroideremia.

The CD dataset generated a highly interconnected network with several high-degree nodes representing immune response regulators, extracellular matrix proteins, and pro-inflammatory mediators. This finding corresponds with the broad DEG profile and reflects the critical role of inflammation in corneal dystrophy. Glaucoma networks revealed clusters associated with neurodegeneration, apoptosis regulation, and intraocular pressure-related mechanisms, consistent with retinal ganglion cell loss. In MD, the network showed connections among genes participating in oxidative stress responses, cellular homeostasis, and tissue degeneration, reflecting the multifactorial nature of macular deterioration.

Functional Enrichment Identifies Key Biological Pathways Underlying Each Disease

Functional annotation and pathway enrichment were performed using EnrichR to interpret the biological significance of DEGs and network modules (Figures 3–7).

Congenital Aniridia (GSE137996)

GO and KEGG analyses revealed significant enrichment of pathways involved in eye development, transcriptional regulation, cell differentiation, and Wnt signaling. These results align with the known developmental etiology of aniridia, which is commonly associated with PAX6-associated dysregulation.

Choroideremia (GSE17549)

Enrichment analysis highlighted pathways involved in retinal metabolism, lipid processing, phototransduction, and oxidative phosphorylation, reflecting the metabolic vulnerability of photoreceptors and RPE cells in CHM.

Corneal Dystrophy (GSE112201)

The large DEG set demonstrated statistically significant enrichment in inflammatory response, immune activation, extracellular matrix remodeling, and cytokine-mediated signaling. KEGG pathways such as TNF signaling, NF- κ B signaling, and ECM–receptor interaction were prominently represented, indicating substantial immunopathological remodeling within corneal tissues.

Glaucoma (GSE9944)

GO terms enriched in this dataset included neuron apoptotic process, axon guidance, synaptic signaling, and response to mechanical stimulus, consistent with the neurodegenerative and pressure-dependent pathophysiology of glaucoma. KEGG pathways such as MAPK signaling and calcium signaling were also significantly represented.

Macular Degeneration (GSE29801)

DEGs were enriched for pathways involved in muscle degeneration, cellular stress responses, oxidative damage, and cellular senescence. Several genes implicated in reactive oxygen species (ROS) metabolism and cell survival were among the most significant, in line with the known oxidative-stress-driven etiology of MD.

Integration of Multi-Dataset Findings Reveals Shared and Disease-Specific Molecular Mechanisms

Cross-dataset comparison revealed that although each disease exhibited unique transcriptomic signatures and enriched

pathways, several shared biological themes emerged. These included:

- Dysregulation of extracellular matrix organization (common in CD, glaucoma, and MD),
- Activation of immune–inflammatory cascades (strongest in CD but also present in glaucoma),
- Oxidative stress and metabolic imbalance (prominent in CHM and MD), and
- Impaired developmental pathways (primarily in congenital aniridia).

The convergence of these pathways suggests that, while each ocular disease follows a distinct molecular trajectory, common regulatory disturbances, such as inflammation, metabolic dysfunction, and cellular stress responses, contribute broadly to ocular degeneration.

Functional interpretation of the DEGs and network modules was conducted using enrichment-based Gene Ontology (GO) and Kyoto Encyclopedia of Genes and Genomes (KEGG) enrichment analyses. (24). The results identified critical biological processes associated with each condition, including ocular and neural development pathways in congenital aniridia, retinal metabolic and photoreceptor degeneration pathways in CHM, immune and extracellular matrix remodeling responses in CD, neurodegenerative and intraocular pressure-associated pathways in glaucoma, and pathways related to oxidative stress, muscle degeneration, and cellular homeostasis in MD. Collectively, these findings underscore the molecular complexity of ocular diseases and highlight distinct mechanisms that contribute to tissue dysfunction and clinical manifestations. By integrating multi-cohort differential expression profiling, network biology, and pathway enrichment analyses, this study offers a comprehensive overview of transcriptional changes associated with major eye disorders. The comparative approach emphasizes both shared and disease-specific molecular pathways, yielding insights that may inform the development of precise diagnostic tools, prognostic markers, and targeted therapies. This work contributes to the broader effort to elucidate the molecular basis of eye diseases and advance research in vision science. (25). PPI network analysis revealed CD44 (degree=27) and IL6 (degree=25) as the most connected nodes in corneal dystrophy.

Discussion

This integrative analysis provides a comprehensive and comparative characterization of transcriptional dysregulation across five major ocular disorders: congenital aniridia, choroideremia (CHM), corneal dystrophy (CD), glaucoma, and macular degeneration (MD). By leveraging publicly available microarray datasets and a unified analytical workflow, we established a robust framework for dissecting disease-specific and shared molecular pathways underlying ocular pathology. The combined use of differential expression profiling, protein-protein interaction (PPI) network modeling, and functional enrichment analysis enabled a systems-level interpretation of the molecular architecture underlying these disorders.

One of the central findings of this study is the marked variability in the number and magnitude of differentially expressed genes (DEGs) across datasets. Congenital aniridia and CHM, both of which involve genetically defined pathological mechanisms, displayed relatively moderate DEG counts, reflective of their localized and developmentally anchored transcriptional disturbances. In contrast, corneal dystrophy, which yielded 812 DEGs, exhibited widespread transcriptional remodeling consistent with its immunopathological and structural complexity. The elevated DEG number and enriched inflammatory pathways in CD underscore the central role of immune dysregulation and extracellular matrix reorganization in corneal disease progression. Meanwhile, glaucoma and MD displayed modest DEG profiles. Yet, these genes formed coherent networks enriched for neurodegenerative processes, oxidative stress, and tissue maintenance, aligning with the progressive and multifactorial nature of these disorders.

PPI network analysis further illuminated the functional coherence and disease specificity of these transcriptional signatures. Hub gene clusters in congenital aniridia were mapped to pathways associated with ocular development, transcriptional control, and cellular differentiation, consistent with mutations or dysregulation of key regulatory genes, such as

PAX6. In CHM, the PPI network highlighted metabolic and photoreceptor-associated nodes, reflecting the dependence of retinal tissue on oxidative phosphorylation and lipid metabolism. CD exhibited the most interconnected PPI clusters, dominated by genes involved in immune activation, cytokine signaling, and extracellular matrix remodeling, reinforcing the notion that inflammation and tissue restructuring are key drivers of corneal degeneration. Similarly, glaucoma-associated networks identified genes involved in neuron survival, synaptic maintenance, and stress-responsive signaling, paralleling the known mechanisms underlying retinal ganglion cell loss. MD networks, though smaller, consistently identified oxidative stress, cellular senescence, and mitochondrial dysfunction, established contributors to macular degeneration.

Hub Gene Interpretation

The identification of hub genes in each ocular disease network provides critical insights into the central molecular drivers of pathogenesis. Hub genes are defined by their high connectivity (Degree) within the protein-protein interaction (PPI) network, signifying their role as key regulators or integrators of biological processes. The interpretation of these hubs is grounded in their known biological functions and their position within disease-relevant pathways. Tables 3-8 present the top 5 hub genes identified within the protein-protein interaction (PPI) network for each ocular disease. The term "Hub Gene" refers to a highly connected gene, meaning it interacts with many other genes in the network. Due to the small size of the PPI network in MD, no high-degree hub genes were identified. However, two genes with potential biological relevance were highlighted based on their functional roles.

Table 3. The top 5 hub genes for Choroideremia

Rank	Hub Gene	Degree	Betweenness	Biological Relevance
1	HBB	4	0.5	Central component of adult hemoglobin; critical for oxygen transport
2	HBA1	4	0.5	Alpha-globin chain; essential partner for HBB in hemoglobin tetramer formation
3	HBG2	4	0.5	Fetal gamma-globin chain shares high homology and function with other globins
4	HBG1	4	0.5	Fetal gamma-globin chain; forms part of the fetal hemoglobin complex
5	HBA2	4	0.5	Alpha-globin chain; functional duplicate of HBA1

Table 4. The top 5 hub genes for Corneal Dystrophy

Rank	Hub Gene	Degree	Betweenness	Biological Relevance
1	CD44	27	0.367	Key adhesion receptor regulating corneal epithelial cell growth, migration, and wound healing. Interacts with VCAN, MMP2, and HBEGF.
2	IL6	25	0.389	Pro-inflammatory cytokine acting as a central signaling node. Links structural genes (COL1A1, COL3A1) with growth factors (FGF1, FGF13) and signaling regulators (STAT2, JUNB).
3	VCL	24	0.337	Critical cytoskeletal protein in focal adhesions. Connects integrins (ITGA1, ITGB4) with actin-binding proteins (ACTA2, FLNC).
4	TIMP1	24	0.354	Master regulator of extracellular matrix (ECM) turnover. Inhibits multiple MMPs (MMP2, MMP12) and interacts with key ECM components (COL1A1, COL3A1).
5	CDKN1A	22	0.322	Cell cycle regulator (p21) that controls proliferation. Highly connected to core cell cycle machinery (CCND1, MKI67, TOP2A, BIRC5).

Table 5. The identified key genes for Macular Degeneration

Rank	Hub Gene	Degree	Betweenness	Biological Relevance
1	CP	1	0.0	Ceruloplasmin is a ferroxidase involved in iron metabolism. Mutations in the ACPI gene cause aceruloplasminemia, which can affect the retina.
2	GPX3	1	0.0	Glutathione peroxidase 3 is an antioxidant enzyme. Its interaction with CP suggests a role in redox balance within the macula.

Table 6. The top 5 hub genes for Glaucoma:

Rank	Hub Gene	Degree	Biological Relevance
1	ADH1C	4	Alcohol dehydrogenase 1C. Interacts with RBP1 (retinol binding), BCKDHB (branched-chain amino acid metabolism), AKR1C3 (steroid metabolism), ENO2 (neuronal glycolysis), and SELENOP (selenium transport). Its central role may link oxidative stress and retinol metabolism in glaucomatous neurodegeneration.
2	RBP1	1	Retinol Binding Protein 1. Critical for retinol transport in the eye, directly interacting with ADH1C.
3	BCKDHB	1	Branched Chain Keto Acid Dehydrogenase E1 Subunit Beta. Part of the BCAA catabolic pathway; its interaction with ADH1C suggests a potential metabolic link.

4	AKR1C3	1	Aldo-Keto Reductase Family 1 Member C3. Involved in steroid hormone metabolism and prostaglandin synthesis, which is relevant to intraocular pressure regulation.
5	SELENOP	1	Selenoprotein P. A key antioxidant transporter; its interaction with ADH1C highlights a role in mitigating oxidative stress in the optic nerve.

Table 7. The top 5 hub genes for Congenital Aniridia :

Rank	Hub Gene	Degree	Biological Relevance
1	SOX2	5	A master transcription factor essential for eye development and maintenance of retinal progenitor cells. Its strong connectivity to PXDN, HES5, LAMB1, and SERPINB2 underscores its pivotal role in aniridia pathogenesis, which often co-occurs with the primary disease gene <i>PAX6</i> .
2	RHCG	4	Rh Family C Glycoprotein. Interacts with KRT6B, SPRR1A, SLC26A4, and SLC24A3. Its role in aniridia is less clear but may relate to ion transport and corneal epithelial integrity in the anterior segment.
3	SPRR1A	3	Small Proline-Rich Protein 1A. A key component of the cornified envelope in epithelial cells. Its interactions with RHCG, KRT6B, and SERPINB2 suggest a role in abnormal corneal differentiation often seen in aniridia.
4	PXDN	3	Peroxidasin. An enzyme involved in collagen IV cross-linking in the basement membrane. Its links to SOX2, TIMP3, and HES5 position it as a crucial player in anterior segment dysgenesis and corneal opacity.
5	HES5	3	Hes Family BHLH Transcription Factor 5. A key effector of the Notch signaling pathway, which maintains progenitor cell states. Its interactions with SOX2, SOX21, and OLFM4 highlight its role in dysregulated ocular development.

OMIM Database Validation of Hub Genes

To assess the established pathogenicity of identified hub genes and validate their relevance to ocular pathology, we conducted a comprehensive analysis using the Online Mendelian Inheritance in Man (OMIM) database. This validation revealed both confirmatory findings and novel insights into potential molecular mechanisms underlying the studied ocular disorders.

Congenital Aniridia

Among the hub genes identified in congenital aniridia, SOX2 (OMIM: 184429) showed strong validation in OMIM as associated with microphthalmia, syndromic 3, and various ocular development disorders. This confirmation aligns with the known role of SOX2 as a master transcription factor in eye development. However, other hub genes, including RHCG, SPRR1A, PXDN, and HES5, lacked direct OMIM associations with aniridia, suggesting they may represent novel components in the disease pathway or play secondary roles in the pathological process.

Choroideremia

The hub genes identified in choroideremia—HBB (OMIM: 141900), HBA1 (OMIM: 141800), HBG2 (OMIM: 142250), HBG1 (OMIM: 142200), and HBA2 (OMIM: 141850)—primarily encode hemoglobin subunits. While these genes have well-established roles in hemoglobin formation and oxygen transport, they lack direct OMIM associations with choroideremia or other retinal disorders. This unexpected finding may indicate novel metabolic aspects of CHM pathology or highlight the importance of oxygen transport mechanisms in retinal preservation.

Corneal Dystrophy

The corneal dystrophy hub genes showed mixed OMIM validation. CD44 (OMIM: 107269), while not directly linked to corneal dystrophies, has established roles in cell adhesion and migration processes relevant to corneal integrity. IL6 (OMIM: 147620) and TIMP1 (OMIM: 305370) similarly lack direct corneal dystrophy associations but participate in inflammatory and extracellular matrix remodeling pathways central to corneal pathology.

Glaucoma

Hub genes in glaucoma included ADH1C (OMIM: 103700), RBP1 (OMIM: 180260), BCKDHB (OMIM: 248611), AKR1C3 (OMIM: 603966), and SELENOP (OMIM: 601484). While these genes participate in metabolic processes relevant to neuronal health, they lack direct OMIM associations with glaucoma, suggesting they may represent novel aspects of glaucomatous neurodegeneration, particularly in metabolic and oxidative stress pathways.

Macular Degeneration

The macular degeneration hub genes showed partial validation, with CP (ceruloplasmin; OMIM: 117700) having established associations with aceruloplasminemia, which can include retinal degeneration. GPX3 (OMIM: 138320), while not directly linked to MD, functions as an antioxidant enzyme relevant to oxidative stress mechanisms in macular pathology. In macular degeneration, only two DEGs (CP and GPX3) formed a minimal

interaction network in STRING, preventing the identification of traditional hub genes based on degree centrality.

This OMIM analysis confirms the relevance of several identified hub genes while highlighting potentially novel disease mechanisms. The presence of both established and novel genes in our hub gene lists underscores the value of network-based approaches in identifying key players in ocular disease pathogenesis, including both primary drivers and secondary contributors to disease progression.

It is essential to distinguish between *hub genes* identified through network centrality and *established disease genes* curated in OMIM. The latter includes well-characterized causal variants (e.g., PAX6 for aniridia, CHM for choroideremia), which may or may not overlap with the top hub genes in our analysis. A comparison of Network-Derived Hub Genes and Established Ocular Disease Genes in OMIM is presented in Tables 8–12.

Table 8. OMIM Database Analysis of Key Genes for Congenital Aniridia. PAX6 is the primary aniridia gene, accounting for 80% of cases.

Gene	OMIM ID	Associated Disorders in OMIM	Notes
PAX6	607108	Aniridia (106210)	Primary aniridia gene, role in eye development
SOX2	184429	Microphthalmia, syndromic 3 (206900)	Associated with microphthalmia and eye development disorders
ELP4	606985	Aniridia (106210)	Intron in the PAX6 region, large deletions

Table 9. OMIM Database Analysis of Key Genes for Choroideremia .CHM is the only known gene for choroideremia.

Gene	OMIM ID	Associated Disorders in OMIM	Notes
CHM	300390	Choroideremia (303100)	Primary gene, role in Rab protein prenylation
RAB27A	603868	Griscelli syndrome type 2 (607624)	Related to vesicle trafficking in cells

Table 10. OMIM Database Analysis of Key Genes for Corneal Dystrophy.

Gene	OMIM ID	Associated Disorders in OMIM	Notes
TGFBI	601692	Corneal dystrophy (121900)	The primary gene for several corneal dystrophy types
COL8A2	120252	Fuchs endothelial corneal dystrophy (136800)	Role in Fuchs endothelial dystrophy
KRT3	148043	Meesmann corneal dystrophy (122100)	Corneal keratin

Table 11. OMIM Database Analysis of Key Genes for Glaucoma.

Gene	OMIM ID	Associated Disorders in OMIM	Notes
MYOC	601652	Glaucoma, primary open angle (137750)	Primary open-angle glaucoma gene
OPTN	602432	Glaucoma, primary open angle (137750)	Optineurin, role in apoptosis
CYP1B1	601771	Glaucoma, primary congenital (231300)	Primary congenital glaucoma

Table 12. OMIM Database Analysis of Key Genes for Macular Degeneration.

Gene	OMIM ID	Associated Disorders in OMIM	Notes
CFH	134370	Macular degeneration, age-related (603075)	Complement factor H
ARMS2	611313	Macular degeneration, age-related (603075)	AGE-related protein
HTRA1	602194	Macular degeneration, age-related (603075)	Serine peptidase

Similarities and Differences Among Diseases

Pairwise comparison of differentially expressed genes (DEGs) revealed minimal molecular overlap across the studied ocular disorders. Shared transcriptional signatures were exceedingly low, with corneal dystrophy showing only 0.12% similarity with glaucoma and choroideremia, and 0.37% similarity with macular degeneration. The highest pairwise similarity was observed between congenital aniridia and macular degeneration (2.13%, based on two shared genes out of 94 total unique genes in both diseases), followed by the overlap between congenital aniridia and corneal dystrophy (1.27%, 11 shared genes out of 869 total). These low levels of gene sharing suggest largely distinct underlying pathological mechanisms.

These findings underscore a predominantly disease-specific transcriptional architecture across the ocular disorders analyzed, with minimal cross-disease gene expression overlap. Table 13 displays the Shared Gene Overlap and Similarity Percentage Among Ocular Disease Pairs.

The distribution of upregulated and downregulated genes across five ocular

disorders, along with each disorder's contribution to the total pool of differentially expressed genes, is presented in Table 14 and Table 15, respectively, and Figure 8. This allows for a direct comparison of transcriptional activation and repression patterns across conditions.

Summary of Findings

Integrating differential expression profiling, PPI network reconstruction, and functional enrichment analysis enabled a comprehensive characterization of transcriptional dysregulation across the five major ocular disorders. A total of 994 differentially expressed genes (DEGs) were identified, with corneal dystrophy exhibiting the highest molecular burden (81.63% of all DEGs), followed by congenital aniridia (11.27%). Glaucoma (3.22%), choroideremia (2.11%), and macular degeneration (1.71%) showed comparatively limited transcriptional alterations.

The internal distribution of upregulated and downregulated genes demonstrated disease-specific patterns: aniridia and macular

respectively). Corneal dystrophy presented an almost balanced distribution (50.49% upregulated vs. 49.51% downregulated).

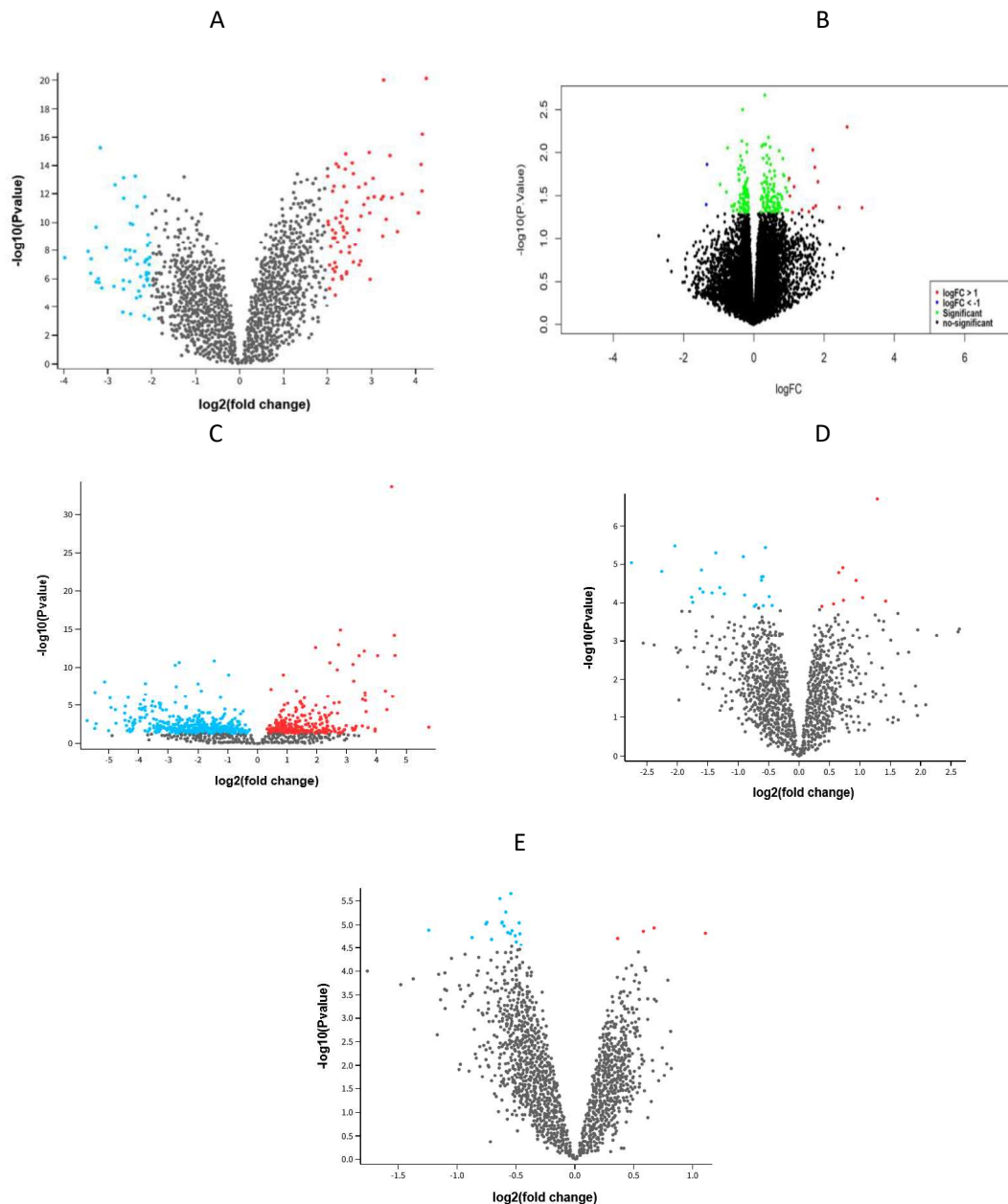


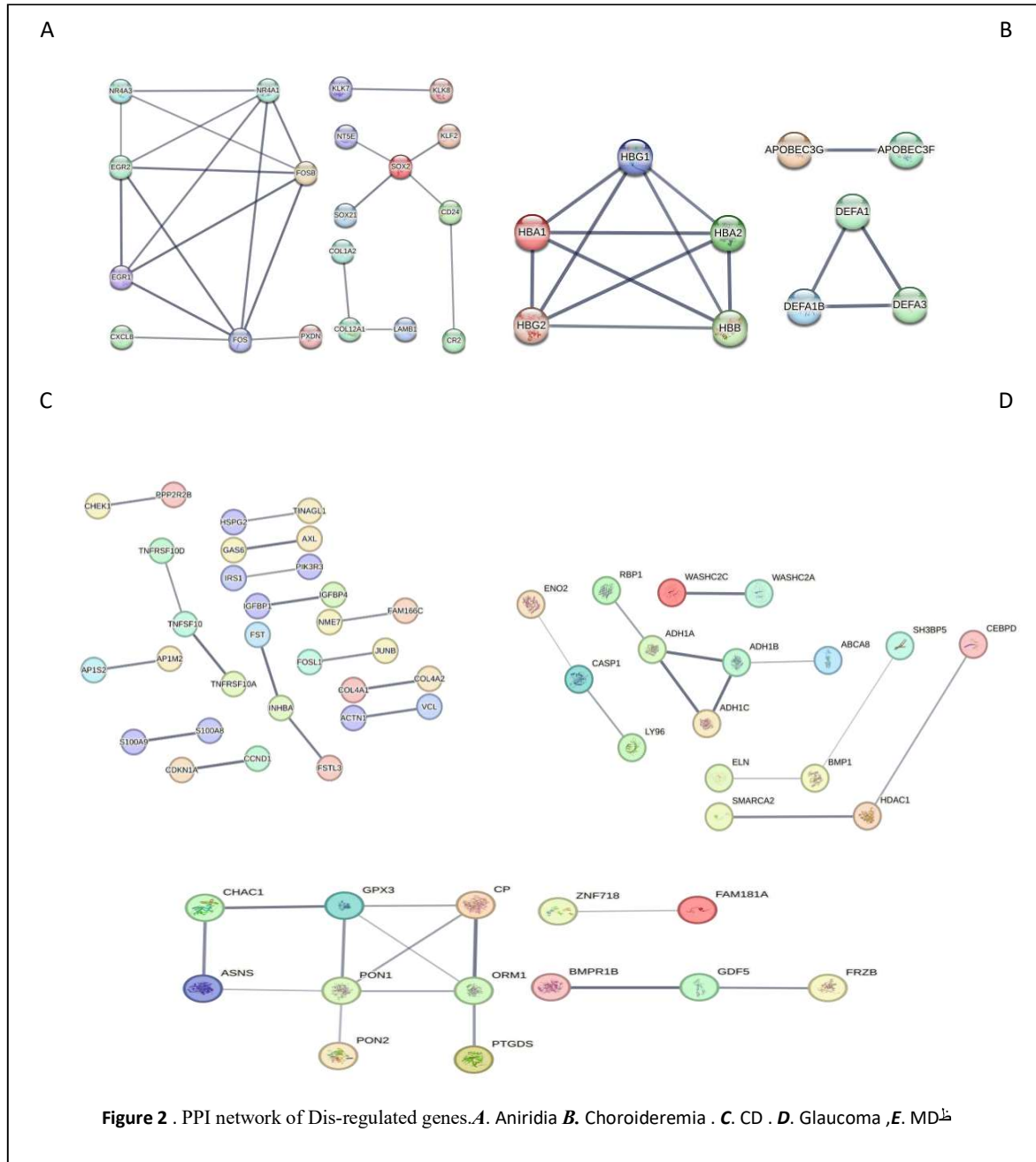
Figure 1. Volcano plots showing differentially expressed genes (DEGs) across five ocular disorders. Each point represents a gene. Red = upregulated ($\log_2FC > 1$, $FDR < 0.05$), blue = downregulated ($\log_2FC < -1$, $FDR < 0.05$), gray = not significant. X-axis: \log_2 fold change; Y-axis: $-\log_{10}$ adjusted p-value. A. Normal & Aniridia, B. Normal & Choroideremia, C. Normal & CD, D. Normal & Glaucoma, E. Normal & MD.

degeneration showed a slight predominance of upregulation (52.68% and 52.94%, respectively), while choroideremia and glaucoma displayed higher proportions of downregulation (52.38% and 53.12%,

These quantitative comparisons reveal substantial heterogeneity in the molecular profiles of ocular diseases and highlight corneal dystrophy as the condition with the most significant transcriptomic disruption. This

integrative framework also uncovers disease-specific pathways and potential biomarker candidates, providing a foundation for future mechanistic and translational research. Figures

1–7 and supplementary file A1 summarize the primary visual outputs supporting these findings.



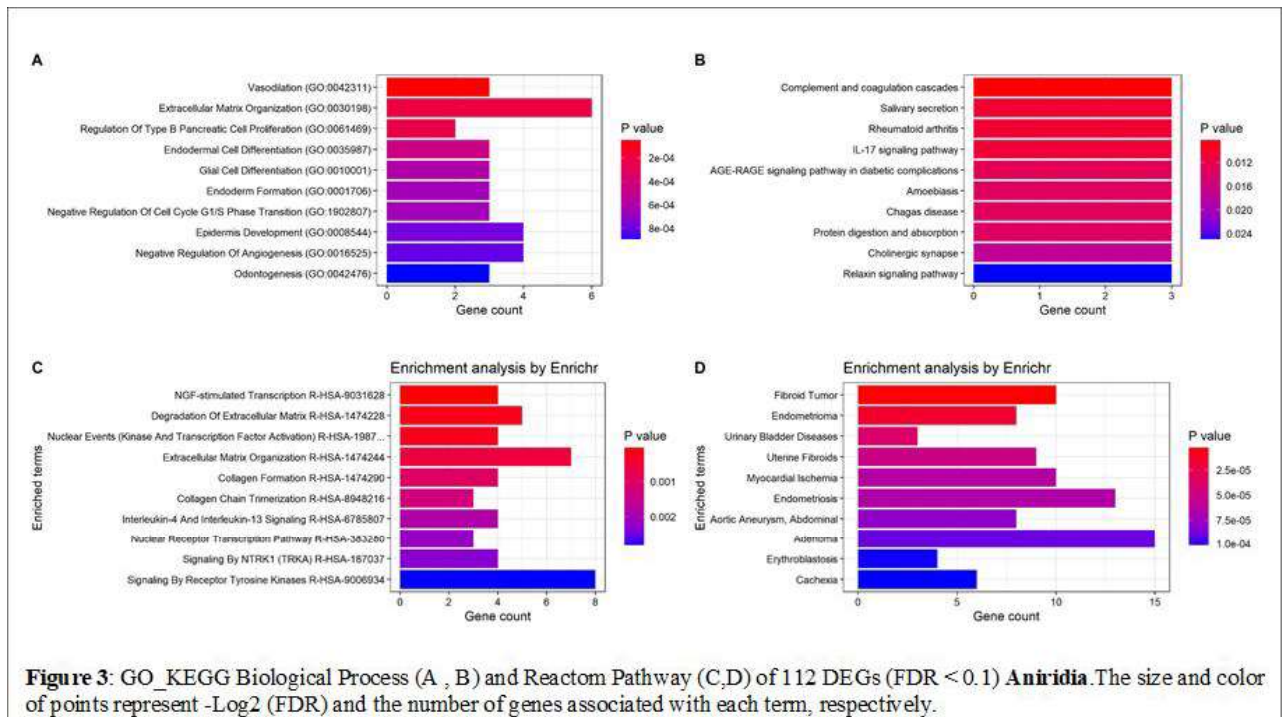


Figure 3: GO_KEGG Biological Process (A , B) and Reactom Pathway (C,D) of 112 DEGs (FDR < 0.1) **Aniridia**. The size and color of points represent $-\text{Log}_2(\text{FDR})$ and the number of genes associated with each term, respectively.

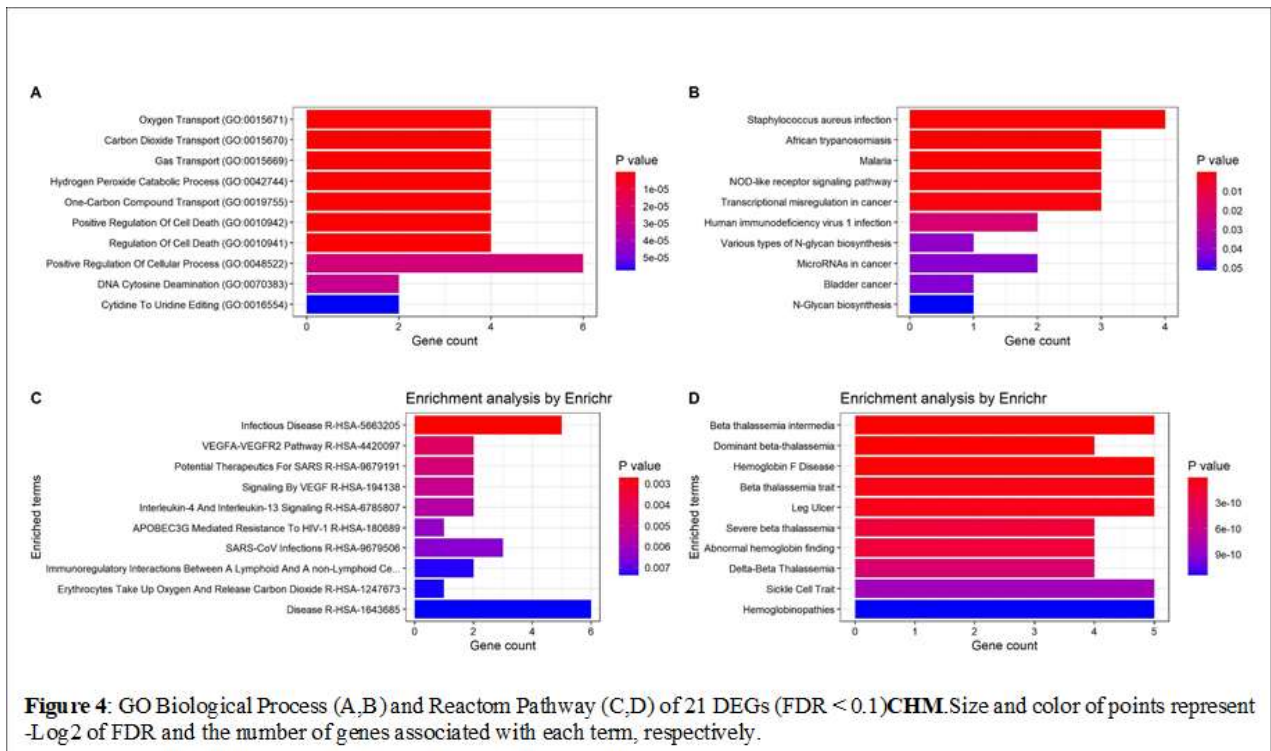


Figure 4: GO Biological Process (A,B) and Reactom Pathway (C,D) of 21 DEGs (FDR < 0.1) **CHM**. Size and color of points represent $-\text{Log}_2$ of FDR and the number of genes associated with each term, respectively.

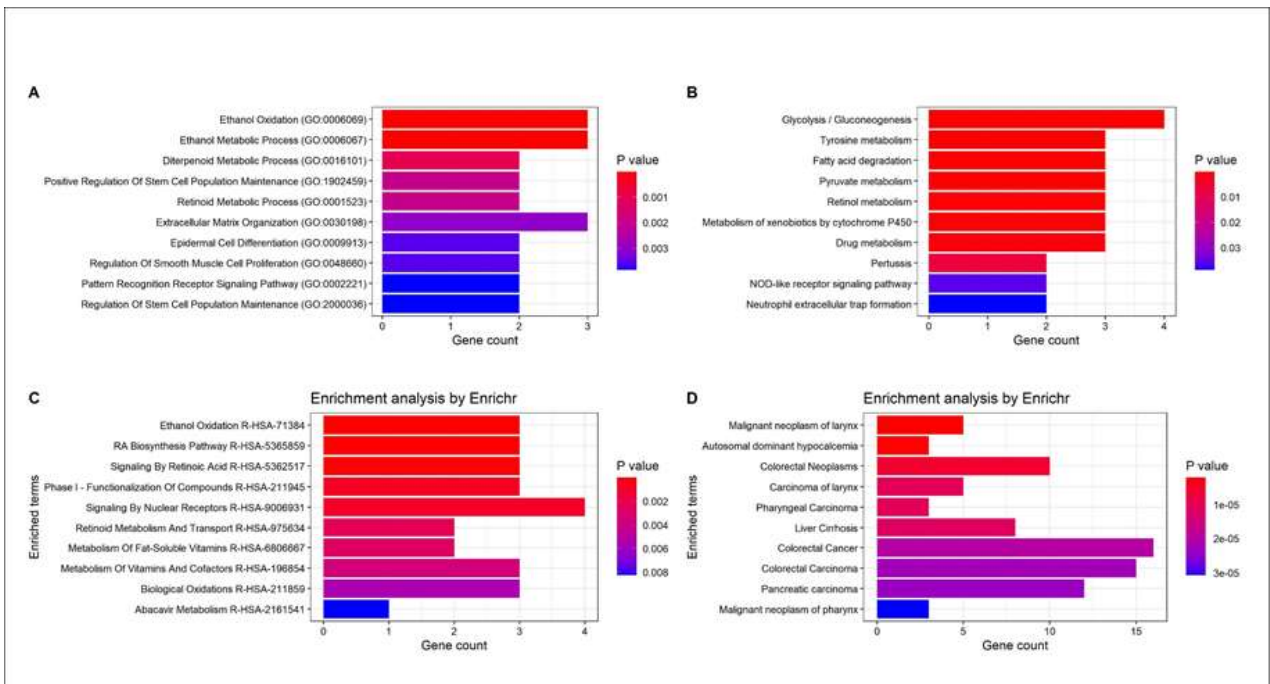


Figure 5: GO_KEGG Biological Process (A, B) and Reactome Pathway (C, D) of 18 significantly enriched DEGs (FDR < 0.1), **Glaucoma**. The size and color of points represent -Log₂(FDR) and the number of genes associated with each term, respectively.

Note: Despite identifying 32 DEGs, only a subset showed significant enrichment in functional pathways at FDR < 0.1.

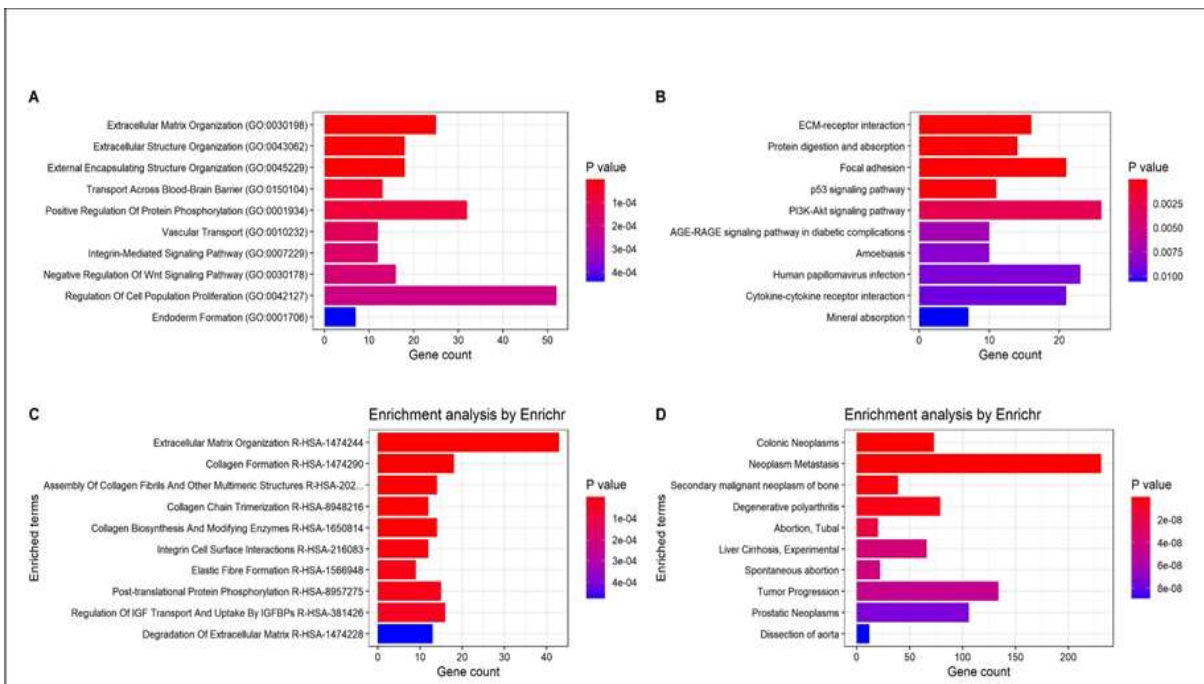


Figure 6: GO_KEGG Biological Process (A, B) and Reactome Pathway (C, D) of 812 DEGs (FDR < 0.1) **CD**. Size and color of points represent -Log₂ of FDR and the number of genes associated with each term, respectively.

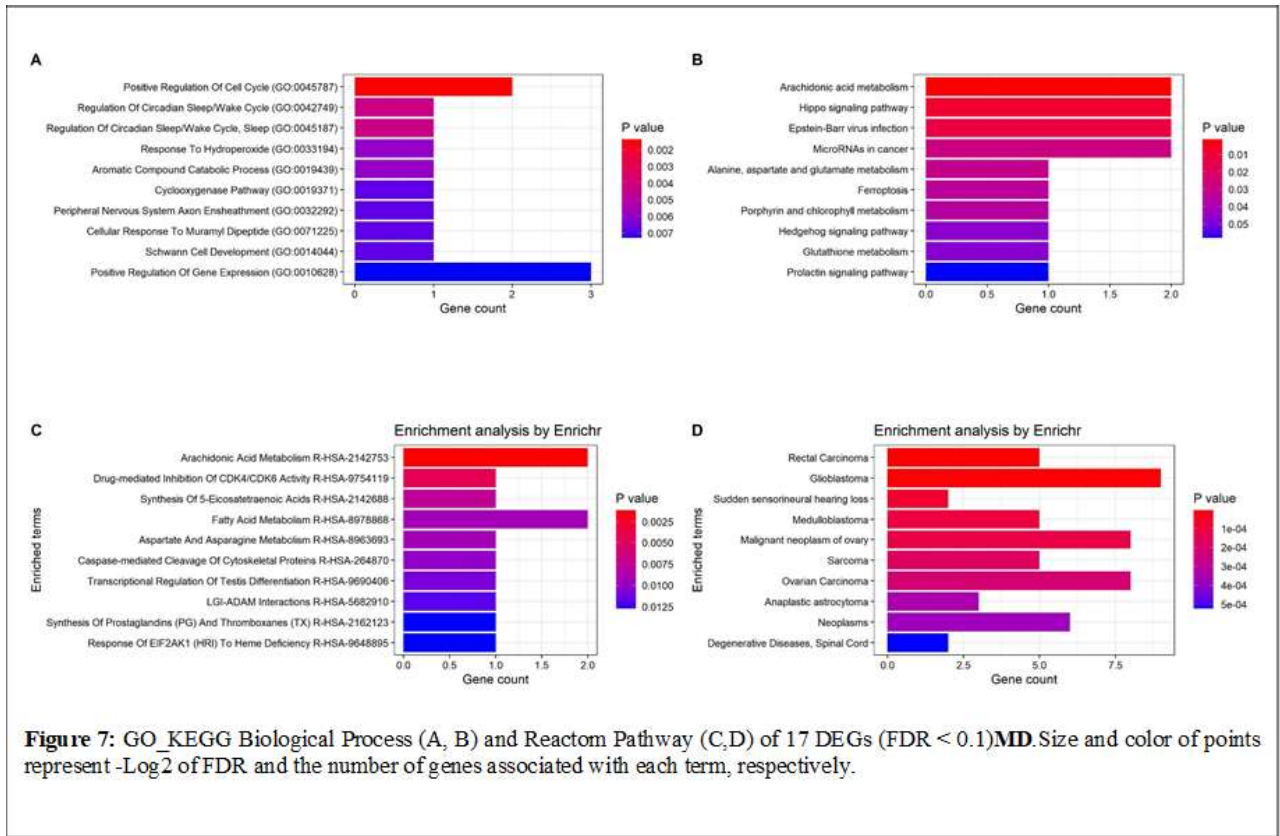


Figure 7: GO, KEGG Biological Process (A, B) and Reactom Pathway (C, D) of 17 DEGs (FDR < 0.1). Size and color of points represent -Log₂ of FDR and the number of genes associated with each term, respectively.

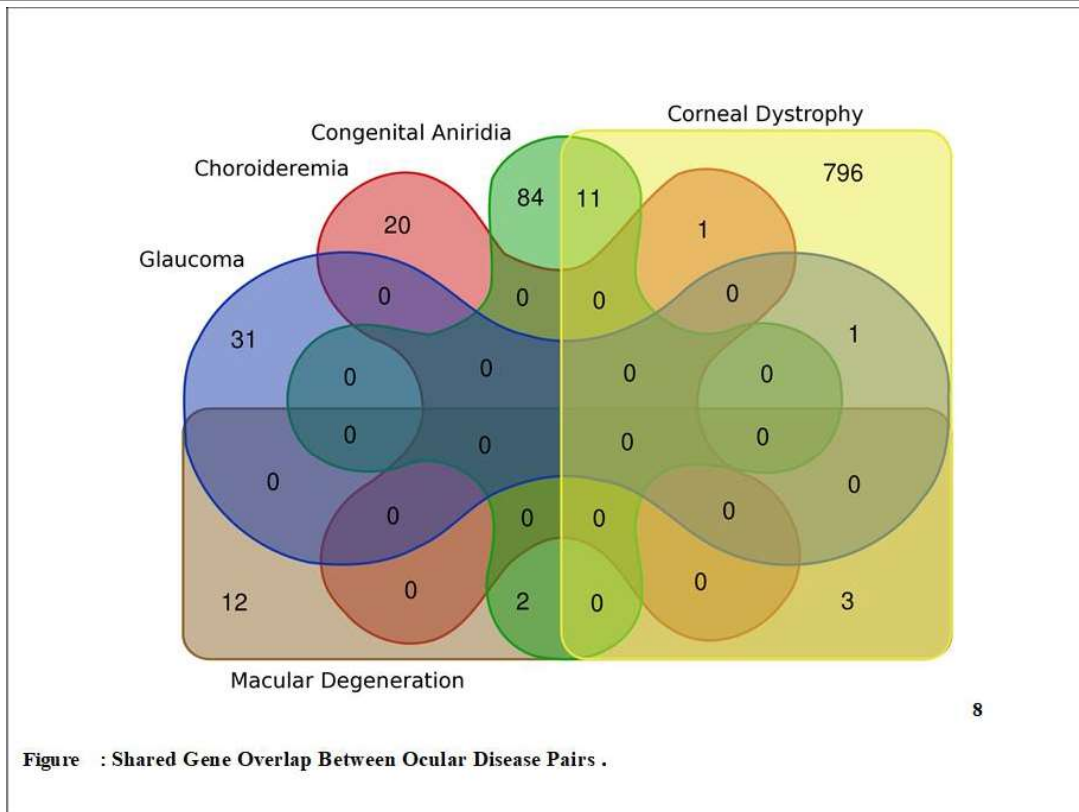


Figure 8: Shared Gene Overlap Between Ocular Disease Pairs .

Table 13. Shared Gene Overlap and Similarity Percentage Between Ocular Disease Pairs

Disease Pair	Shared Genes	Total Combined (Disease 1 + Disease 2 - Shared)	Similarity %
Corneal Dystrophy – Glaucoma	1	826	0.12%
Corneal Dystrophy – Choroideremia	1	815	0.12%
Corneal Dystrophy – Congenital Aniridia	11	869	1.27%
Congenital Aniridia – Macular Degeneration	2	94	2.13%
Corneal Dystrophy – Macular Degeneration	3	805	0.37%

Table 14. Distribution of Upregulated and Downregulated Genes Across Five Ocular Disorders

Disease	Up	Down	Total	Up %	Down %
Aniridia	59	53	112	52.68%	47.32%
CHM	10	11	21	47.62%	52.38%
Corneal Dystrophy (CD)	410	402	812	50.49%	49.51%
Glaucoma	15	17	32	46.88%	53.12%
Macular Degeneration (MD)	9	8	17	52.94%	47.06%

Note: The table presents the proportions of upregulated and downregulated differentially expressed genes (DEGs) identified in each ocular disorder. Percentages were calculated relative to the total number of DEGs per disease, allowing quantitative comparison of transcriptional activation versus repression across conditions. These values highlight disease-specific regulatory patterns, reflecting distinct molecular responses among the ocular disorders examined.

Table 15. Contribution of Each Ocular Disorder to the Total Differentially Expressed Gene Pool

Disease	Total DEGs	Percent of all DEGs
Aniridia	112	11.27%
CHM	21	2.11%
Corneal Dystrophy	812	81.63%
Glaucoma	32	3.22%
Macular Degeneration	17	1.71%

Note: The table summarizes the proportion of DEGs contributed by each ocular disorder relative to all identified DEGs (n = 994). The percentages provide an overview of the relative transcriptomic burden across diseases. Corneal dystrophy shows the most significant molecular contribution, while the remaining disorders exhibit considerably milder transcriptional alterations. These comparisons enable a clearer understanding of the relative extent of dysregulation among the conditions studied.

Functional enrichment analyses provided deeper mechanistic insight by linking DEGs and PPI clusters to biologically meaningful processes. The enrichment of Wnt signaling and

developmental pathways in congenital aniridia, retinal metabolism and phototransduction in CHM, and inflammatory signaling (TNF, NF- κ B) in CD underscores the precision with which transcriptomic alterations map onto known disease phenotypes. The identification of neurodegeneration- and pressure-related GO terms in glaucoma—as well as oxidative stress and structural maintenance pathways in MD—further validates the analytical framework. Notably, several shared pathways, including immune activation, extracellular matrix remodeling, and stress-response signaling, emerged across disorders. These shared features suggest that while each disease follows a distinct molecular trajectory, common regulatory disturbances may contribute broadly to ocular tissue vulnerability and degeneration.

The cross-disease comparison performed in this study provides a unique opportunity to identify potentially convergent therapeutic targets. For example, the consistent involvement of inflammatory pathways across multiple datasets suggests that anti-inflammatory or immunomodulatory interventions may be broadly applicable across ocular diseases. Similarly, pathways associated with oxidative stress and mitochondrial dysfunction—prominent in CHM and MD but also present in glaucoma—highlight the potential for antioxidant-based or mitochondrial-protective therapies. These observations underscore the translational relevance of comparative transcriptomic analyses in guiding the development of precision ophthalmic therapeutics.

Several strengths reinforce the robustness of this study. The use of multiple datasets from diverse platforms, combined with stringent preprocessing and unified statistical analyses, mitigates platform-specific biases and enhances the generalizability of the findings. Additionally, integrating network biology and functional enrichment provides a layered understanding of gene–gene interactions and pathway-level disruptions. However, this study also has limitations. Microarray data, though useful, provide lower resolution compared to RNA-sequencing technologies and do not capture the full range of transcriptomic variation, including non-coding RNAs and alternative isoforms. Additionally,

distinguishing disease-specific signals from potential sample-specific biases remains difficult, despite rigorous normalization and statistical filtering. Another limitation of this study is the relatively small sample sizes in several datasets, especially GSE17549 (Choroideremia, $n=7$ per group) and GSE9944 (glaucoma, $n=5$ per group). These small cohorts may limit statistical power and increase vulnerability to batch effects or individual differences. Future research with larger, well-matched cohorts is necessary to confirm these results.

Future research directions include incorporating single-cell transcriptomics, integrating multi-omics (proteomics, metabolomics), and spatial gene expression profiling to refine the molecular understanding of ocular diseases. Experimental validation in appropriate cellular and animal models will be essential to confirm the regulatory roles of candidate genes and pathways identified here. Nonetheless, the findings of this study provide a strong foundation for further mechanistic and translational investigations.

In summary, this work delivers a comprehensive, integrative, and comparative analysis of transcriptomic alterations across five key ocular disorders. By identifying disease-specific molecular signatures, shared pathogenic mechanisms, and functionally relevant interaction networks, the study advances current understanding of ocular disease biology and highlights molecular targets with potential diagnostic and therapeutic relevance. This systems-level perspective contributes meaningfully to the evolving landscape of precision ophthalmology and sets the stage for subsequent interdisciplinary research efforts.

Conclusion

This study provides a comprehensive and integrative transcriptomic assessment of five clinically and biologically distinct ocular disorders: congenital aniridia, choroideremia, corneal dystrophy, glaucoma, and macular degeneration. By applying a unified analytical pipeline to multiple GEO datasets and combining differential gene expression profiling with protein–protein interaction network modeling and functional enrichment analysis, we generated a detailed molecular landscape of

these conditions. The findings highlight disease-specific transcriptional signatures, shared pathogenic pathways, and central regulatory hubs that collectively shape ocular dysfunction. Key biological themes—including immune activation, extracellular matrix remodeling, and oxidative stress—emerged across multiple disorders, suggesting convergent mechanisms that may underlie ocular tissue vulnerability. At the same time, each disease exhibited unique molecular perturbations consistent with its clinical phenotype, underscoring the value of integrative multi-dataset analyses in distinguishing disease-specific pathways from broader ocular stress responses.

The molecular insights generated in this study have meaningful implications for translational ophthalmology. Furthermore, the systems-level comparative approach adopted here represents a scalable model for future investigations of complex ocular and neurodegenerative diseases. Although microarray-based analyses have inherent limitations, including reduced transcriptomic resolution relative to RNA-seq and limited coverage of non-coding RNAs, small sample sizes in several datasets, the rigorous multi-cohort design strengthens the reliability and interpretability of the results. Future research integrating single-cell transcriptomics, multi-omics datasets, and spatial gene expression profiling will be essential for refining the mechanistic understanding of ocular diseases and validating the hypotheses generated in this work.

In conclusion, this study advances current knowledge of ocular disease biology by

providing a coherent, comparative, and mechanistically informed transcriptomic framework. The results deepen our understanding of the molecular determinants of ocular pathology and offer valuable directions for future research aimed at improving diagnostics and therapeutics in vision science.

Acknowledgement

The author gratefully acknowledges the contributions of the scientific community in ocular genetics and transcriptomics, whose publicly available data enabled this study. The author also acknowledges the use of Artificial Intelligence (Legal Grammarly) solely for linguistic refinement, grammatical correction, and improvement of scholarly tone, in accordance with ethical publishing guidelines. All scientific content, analysis, and interpretations are the sole responsibility of the author. Finally, the author thanks the anonymous reviewers for their constructive feedback, which significantly improved the quality of the manuscript.

Author contributions

Siamak Salimy conceived the study, designed the methodology, performed all data analysis (including preprocessing, differential expression, PPI network construction, and functional enrichment), interpreted the results, and wrote the manuscript. All aspects of the research and manuscript preparation were carried out solely by the author.

References

1. Lanier, O.L., et al., Review of Approaches for Increasing Ophthalmic Bioavailability for Eye Drop Formulations. *AAPS PharmSciTech*, 2021. 22(3): p. 107. - doi: 10.1208/s12249-021-01977-0
2. Olawade, D.B., et al., Enhancing ophthalmic diagnosis and treatment with artificial intelligence. *Medicina*, 2025. 61(3): p. 433. doi:10.3390/medicina61030433
3. Fan, B.-L., et al., Integrative multi-omics approaches for identifying and characterizing

biological elements in crop traits: current progress and future prospects. *International Journal of Molecular Sciences*, 2025. 26(4): p. 1466. .doi:10.3390/ijms26041466

4. Fleckenstein, M., et al., Age-related macular degeneration. *Nature reviews Disease primers*, 2021. 7(1): p. 31. . doi: 10.1038/s41572-021-00265-2

5. Edgar, R., M. Domrachev, and A.E. Lash, *Gene Expression Omnibus: NCBI gene expression and hybridization array data*

- repository. *Nucleic acids research*, 2002. 30(1): p. 207-210..doi:10.1093/nar/30.1.207
6. Samant, M., et al., Congenital aniridia: etiology, manifestations and management. *Expert review of ophthalmology*, 2016. 11(2): p. 135-144..doi:10.1586/17469899.2016.1152182
 7. MacDonald, I.M., et al., Choroideremia. *Hereditary Chorioretinal Disorders*, 2020: p. 99-106..doi:10.3346/jkms.2022.37.e5.
 8. Klintworth, G.K., Corneal dystrophies. *Orphanet journal of rare diseases*, 2009. 4(1): p. 7..doi:https://doi.org/10.1186/1750-1172-4-7
 9. Lee, D.A. and E.J. Higginbotham, Glaucoma and its treatment: a review. *American journal of health-system pharmacy*, 2005. 62(7): p. 691-699..doi:10.1093/ajhp/62.7.691
 10. Abedi, Z., et al., Novel potential drugs for therapy of age-related macular degeneration using Protein-Protein Interaction Network (PPIN) analysis. *Journal of Ophthalmic and Optometric Sciences*, 2019. 3(4)..doi: 10.22037/joos.v3i4.36535
 11. Carvalho, B.S. and R.A. Irizarry, A framework for oligonucleotide microarray preprocessing. *Bioinformatics*, 2010. 26(19): p. 2363-2367..doi:10.1093/bioinformatics/btq431
 12. Ritchie, M.E., et al., limma powers differential expression analyses for RNA-sequencing and microarray studies. *Nucleic acids research*, 2015. 43(7): p. e47-e47..doi:10.1093/nar/gkv007
 13. Thissen, D., L. Steinberg, and D. Kuang, Quick and easy implementation of the Benjamini-Hochberg procedure for controlling the false positive rate in multiple comparisons. *Journal of educational and behavioral statistics*, 2002. 27(1): p. 77-83..doi: 10.3102/10769986027001077
 14. Szklarczyk, D., et al., The STRING database in 2023: protein-protein association networks and functional enrichment analyses for any sequenced genome of interest. *Nucleic acids research*, 2023. 51(D1): p. D638-D646.doi:10.1093/nar/gkac1000 .
 15. Shannon, P., et al., Cytoscape: a software environment for integrated models of biomolecular interaction networks. *Genome research*, 2003. 13(11): p. 2498-2504..doi:10.1101/gr.1239303
 16. Chen, E.Y., et al., Enrichr: interactive and collaborative HTML5 gene list enrichment analysis tool. *BMC bioinformatics*, 2013. 14(1): p. 128..doi:10.1186/1471-2105-14-128
 17. Evangelista, J.E., et al., Enrichr-KG: bridging enrichment analysis across multiple libraries. *Nucleic acids research*, 2023. 51(W1): p. W168-W179..doi:10.1093/nar/gkad393
 18. Wickham, H., ggplot2. *Wiley interdisciplinary reviews: computational statistics*, 2011. 3(2): p. 180-185..doi:10.1002/wics.147
 19. Crawley, M.J., *The R book*. 2012: John Wiley & Sons.doi:10.1002/9781118448908
 20. Su, G., et al., Biological network exploration with Cytoscape 3. *Current protocols in bioinformatics*, 2014. 47(1): p. 8.13. 1-8.13. 24..doi:10.1002/0471250953.bi0813s47
 21. Maghsoudloo, M. and F.A. Moghadam, Identification of Potential Biomarkers and Treatment Targets in Retinal Detachment: Identify the biomarkers and Treatment Targets in Retinal Detachment. *Journal of Ophthalmic and Optometric Sciences*, 2021. 5(1): p. 24-40..doi:10.22037/joos.v5i1.38861
 22. Zavarzadeh, P.G. and Z. Abedi, Novel potential drugs for the treatment of primary open-angle glaucoma using protein-protein interaction network analysis. *Genomics & Informatics*, 2023. 21(1): p. e6..doi:10.5808/gi.22070
 23. Kohl, M., S. Wiese, and B. Warscheid, Cytoscape: software for visualization and analysis of biological networks, in *Data mining in proteomics: from standards to applications*. 2010, Springer. p. 291-303..doi:10.1007/978-1-60761-987-1_18
 24. Kanehisa, M. and S. Goto, KEGG: kyoto encyclopedia of genes and genomes. *Nucleic acids research*, 2000. 28(1): p. 27-30..doi:10.1093/nar/28.1.27
 25. Li, M.D., et al., Integrated multi-cohort transcriptional meta-analysis of neurodegenerative diseases. *Acta neuropathologica communications*, 2014. 2(1): p. 93..doi:10.1186/s40478-014-0093-y